

# Articles

## Structural and Transport Properties of Mixed Phosphotungstic Acid/Phosphomolybdic Acid/SiO<sub>2</sub> Glass Membranes for H<sub>2</sub>/O<sub>2</sub> Fuel Cells

Thanganathan Uma and Masayuki Nogami\*

Department of Materials Science and Engineering, Nagoya Institute of Technology,  
Showa, Nagoya 466-8555, Japan

Received March 1, 2007. Revised Manuscript Received May 22, 2007

The synthesis and characterization of a novel inorganic glass composite membrane consisting of a mixture of phosphotungstic acid and phosphomolybdic acid are reported. Phosphosilicate gels doped with these two proton conducting donor components were derived by a sol–gel method. The influence of the textural properties of the glass composites could be interpreted from N<sub>2</sub> adsorption–desorption isotherms. The pore size was less than 6 nm for all glass membranes. These glass membranes were found to be stable up to 400 °C. Fourier transform infrared spectroscopy indicated that the characteristic Keggin anions PW<sub>12</sub>O<sub>40</sub><sup>3–</sup> and PMo<sub>12</sub>O<sub>40</sub><sup>3–</sup> were present in the glass composite membrane. The highest proton conductivity was measured to 1.01 × 10<sup>–1</sup> S cm<sup>–1</sup> at 85 °C with 85% relative humidity (RH). Membrane electrode assemblies were prepared and showed good performance, with a maximum power density value of 35 mW/cm<sup>2</sup> at 93 mA/cm<sup>2</sup> as well as a current density of 137 mA/cm<sup>2</sup> when utilized in a H<sub>2</sub>/O<sub>2</sub> fuel cell at 28 °C and 30% RH.

### Introduction

Proton conductive solids are favorable materials as solid electrolytes for fuel cells. In recent years, extensive efforts have been dedicated to the research and development of new electrolytic membranes for fuel cell applications. However, some limitations exist in their utilization at temperatures above 100 °C,<sup>1</sup> and furthermore, fuel cells operating at the usual temperatures of 70–90 °C experience a short lifetime if hydrogen containing trace amounts of carbon monoxide (CO) is used.<sup>2</sup> The short lifetime is a result of CO acting as a strong poison for the anode catalyst at low temperature,<sup>3</sup> and CO is always present in hydrogen obtained from the reforming process of light hydrocarbons or methanol. On the other hand, the use of pure hydrogen, obtained by an electrolytic process, is not an economically viable option.

Heteropolyacids (HPAs) are a class of inorganic proton conducting materials known to possess high proton conductivities at room temperature. The ability of these compounds to retain water even at high temperatures and act as superacids makes them excellent proton conductors, and membranes with enhanced proton conduction equates greater

power outputs from the fuel cell. There are three main commercially produced HPAs: 12-phosphotungstic acid, 12-phosphomolybdic acid, and 12-silicotungstic acid. These compounds have been studied at great length by many other research groups, and this is the reason we have decided to focus mainly on non-commercial HPAs. Certain proton conductors, such as HPAs and protonic acids, become dehydrated or thermally decomposed at medium-ranged temperatures and relatively low humidity, whereas the thermal stability of an HPA can be improved by incorporating it into a modified silica matrix under high humidity.<sup>4–6</sup> Therefore, a combination of matrices with a good affinity for adsorbed water is a key point to satisfy the requirements for solid-state proton conductors employed at medium-ranged temperatures and low levels of humidity.<sup>7,8</sup>

Heteropoly compounds are efficient, solid, “super”-acid catalysts for a wide variety of reactions.<sup>9,10</sup> It is known that various polar molecules are easily incorporated into the bulk of H<sub>3</sub>PW<sub>12</sub>O<sub>40</sub> (phosphotungstic acid, PWA) and catalyzed by protons in the bulk, a so-called “pseudoliquid” catalytic

\* Corresponding author. Tel.: +81 52 735 5285. Fax: +81 52 735 5285  
E-mail: nogami@mse.nitech.ac.jp.

- (1) Kreuer, K. D. *Solid State Ionics* **1997**, 97, 1.
- (2) Kadowaki, M.; Taniguchi, S.; Akiyama, Y.; Miyake, Y.; Matsubayashi, T.; Nishio, K. *Abstracts of 1998 Fuel Cell seminar*, Palm Springs, CA, Nov. 16–17, 1998; p 326.
- (3) Schmidt, T. J.; Gasteiger, H. A.; Behm, R. J. *J. New Mater. Electrochem. Syst.* **1999**, 2, 27.

- (4) Moffat, J. B. *Metal-Oxygen Clusters*; Kluwer Academic/Plenum Press: New York, 2001.
- (5) Sadakane, M.; Steckhan, E. *Chem. Rev.* **1998**, 98, 219.
- (6) Savadogo, O.; Barolacci, G. *Int. J. Hydrogen Energy* **1992**, 17, 109.
- (7) Savadogo, O.; Essalik, A. U.S. Patent 5,298,343, 1994.
- (8) Hocevar, S.; Staiti, P.; Giordano, N. *Proceedings of the International Symposium on New Materials for Fuel Cells and Modern Battery Systems II*, Montreal, Canada, July 6–10, 1997; p 297.
- (9) Okuhara, E. G. T.; Mizuno, N.; Misono, M. *Adv. Catal.* **1996**, 41, 113.
- (10) Misono, M. *Catal. Rev. Sci.-Eng.* **1987**, 29, 269.

process. Water molecules are also incorporated into the bulk to form stable hydrates. The catalytic activity of PWA changes with the number of water molecules in the bulk ( $n$  in  $\text{HPW} \cdot n\text{H}_2\text{O}$ ),<sup>11</sup> and hence, interactions between  $\text{H}^+$  and water molecules are of great concern for the understanding of its acidity and catalytic activity. It has been confirmed by X-ray diffraction (XRD) and neutron diffraction that, at  $n = 6$ ,  $\text{H}^+$  is associated with two water molecules to form a  $\text{H}_5\text{O}_2^+$  cation connecting HPW anions.<sup>12</sup> Unfortunately though, IR spectra of OH band of HPAs with varying water content are not well understood.

HPAs have been studied at the Institute CNR-TAE,<sup>13–15</sup> and the investigations have shown that the PWA (or HPA compounds) utilized in hydrogen/oxygen fuel cells gave power density values of about  $700 \text{ mW/cm}^2$ .<sup>13</sup> Moreover, the HPA had a protective effect against the CO poisoning of the platinum catalyst present at the anode<sup>16</sup> and exhibited a promoting effect on the electrochemical reduction of oxygen at the cathode.<sup>13</sup> In the fuel cell test, the acid was utilized in its crystalline state thus giving rise to some problem during endurance tests. In fact, the electrolyte in its solid form was dissolved in the electrochemically produced water that leaked out through the gas outlet tubes, leading to the dissolved electrolyte flooding the electrodes and creating gas diffusion problems. For these reasons, it was thought that an interesting approach would be to anchor the HPA to a stable support in such a way that it would not be washed away by the water generated in the fuel cell but rather that it would retain, as much as possible, its conductive characteristics. Silicotungstic acid was preferred to PWA because it can be supported on silica to a larger extent.<sup>17</sup>

The acid  $\text{H}_3\text{PW}_{12}\text{O}_{40}$  (abbreviated as  $\text{H}_3\text{PW}$ ) was selected for a study because it has been reported to be the strongest acid in the series. It is commercially available as a crystalline hydrate and has been thoroughly studied and reviewed.<sup>18–22</sup> Molybdophosphoric acid and its analogues are highly conductive as long as they contain large amounts of water in the crystal structure and hence are so sensitive to humidity that a difficulty similar to that observed for liquid electrolyte fuel cells arises.<sup>23,24</sup> These are composite materials with inorganic acidic nanoparticles incorporated within a host glass electrolyte membrane such as PWA or phosphomo-

lybdic acid (PMA). The target operating fuel cell temperature in this work is below  $50^\circ\text{C}$  with a relative humidity (RH) around 30%. Recently, we have synthesized and characterized HPAs (i.e., PMA and PWA) doped to a phosphosilicate glass membrane<sup>25,26</sup> for  $\text{H}_2/\text{O}_2$  fuel cell electrolytes. A maximum proton conductivity of  $9.1 \times 10^{-2} \text{ S cm}^{-1}$  at  $90^\circ\text{C}$  and a good cell performance (i.e., a power density =  $22.9 \text{ mW/cm}^2$ ) were obtained at low temperature. As a continuation to these studies, we wish to prepare a new class of glass membranes consisting of a phosphosilicate matrix doped with a mixture of PWA and PMA.

The present work deals with the synthesis and characterization of glass composites based on a highly proton conductive structure as obtained by mixing PWA and PMA. The influence of PWA and PMA on the structure, proton conductivity, permeability, and fuel cell performance was investigated. The interaction of protonic species with Keggin anions was discussed. Preliminary results of the crystal structure indicate that it was composed of Keggin anions and phosphosilicate composites. The new technology based on nanopore glass composite membranes was expected to raise the output density of the  $\text{H}_2/\text{O}_2$  fuel cell system. The current electrolyte material of choice for  $\text{H}_2/\text{O}_2$  fuel cells was glass, because this material, derived by a sol–gel method, allows for a current output greater than  $100 \text{ mA/cm}^2$ . One of the goals was to find a membrane that could produce a current equal to or greater than that of Nafion but at room temperature.

## Experimental Techniques

**Materials.** The HPAs  $\text{H}_3\text{PW}_{12}\text{O}_{40}$  (PWA, Aldrich) and  $\text{H}_3\text{PMo}_{12}\text{O}_{40}$  (PMA, Kishida chemicals) as well as diisopropylphosphate (Wako) and  $N,N$ -dimethylformamide (99%, Kishida chemicals) were utilized without further purification. Solvents and reagents of analytical grade were commercial products and were used as received. Water purified with a Milli-Q system from Millipore (AQUARIUS/GS-20R, Japan) was used for the experiments. Poly(tetrafluoroethylene) (Aldrich, 60% dispersion in water), Pt/C powder (Tanaka, Kikinzoku, Kogyo K.K.), Nafion perfluorinated ion-exchange resin, (Aldrich), and a 0.2 mm diameter Pt wire (Aldrich) were all used as received.

**Preparation and Evaluation of the Electrode/Electrolyte.** Glass composite membranes and electrodes were prepared with a procedure similar to that developed by our research group for  $\text{H}_2/\text{O}_2$  fuel cells.<sup>25,26</sup> The electrodes for  $\text{H}_2/\text{O}_2$  fuel cells were made from approximately 0.20 mm thick carbon sheets coated with an approximately 0.01–0.03 mm thick catalytic layer with a loading of  $0.1 \text{ mg/cm}^2$  Pt/C. This resulted in a total electrode thickness of approximately 0.21–0.23 mm. The membrane electrode assembly (MEA) consisted of the glass composite membrane (0.55 mm thick) sandwiched between the anodic and cathodic catalytic layers, giving rise to an active area of  $0.25 \text{ cm}^2$ . The MEA was sandwiched between glass pieces and the Pt/C electrodes and tightened with two platinum meshes connected by lengthy platinum wire to the anode and cathode sections, respectively. The performance of the fuel cell was studied with respect to the humidity of the gas streams by external as well as membrane humidification.

**Characterization of the Glass Composite Membrane.**  $\text{N}_2$  adsorption–desorption isotherms were measured on a Quantochrome

- (11) Okuhara, E. G. T.; Hashimoto, T.; Hibi, T.; Misono, M. *J. Catal.* **1985**, 93, 224.
- (12) Brown, G. M.; Nnoe-Spirlet, M. R.; Busing, W. R.; Levy, H. A. *Acta Crystallogr.* **1977**, B33, 1038.
- (13) Giordano, N.; Arico, A. S.; Hocevar, S.; Staiti, P.; Antonucci, P. L.; Antonucci, V. *Electrochim. Acta* **1993**, 38, 1733.
- (14) Giordano, N.; Staiti, P.; Hocevar, S.; Arico, A. S. *Electrochim. Acta* **1996**, 41, 397.
- (15) Staiti, P.; Hocevar, S.; Hocevar, S. *Int. J. Hydrogen Energy* **1997**, 22, 809.
- (16) Hocevar, S.; Staiti, P. In *Proceedings of the 3rd International symposium on Electrocatalysis, Advances and Industrial Applications*, Portoroz-Portorose, Slovenia, Sept 11–15, 1999; Hocevar, S., Gasberscek, M., Pinter, A., Eds.; p 232.
- (17) Staiti, P.; Freni, S.; Hocevar, S. *J. Power Sources* **1999**, 79, 250.
- (18) Tatsumisago, M.; Minami, T. *J. Am. Ceram. Soc.* **1989**, 72, 484.
- (19) Tatsumisago, M.; Honjo, H.; Sakai, Y.; Minami, T. *Solid State Ionics* **1994**, 74, 105.
- (20) Okuhara, T.; Mizuno, N.; Misono, M. *Adv. Catal.* **1996**, 41, 113.
- (21) Kozhevnikov, I. V. *Catal. Rev. Sci.-Eng.* **1995**, 37, 311.
- (22) Hill, C. L.; McCartha, C. M. P. *Coord. Chem. Rev.* **1995**, 143, 407.
- (23) Corma, A. *Chem. Rev.* **1995**, 95, 559.
- (24) Tsigdinos, G. A. *Top. Curr. Chem.* **1978**, 76, 1.

- (25) Uma, T.; Nogami, M. *J. Electrochem. Soc.* **2007**, 154, B32.
- (26) Uma, T.; Nogami, M. *J. Membr. Sci.* **2006**, 280, 744.

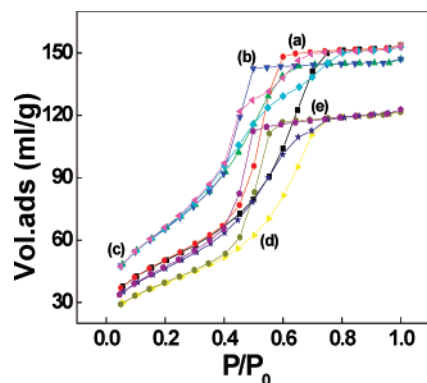


**Figure 1.** Nitrogen adsorption-desorption plots of PWA/PMA- $P_2O_5$ - $SiO_2$  glass sample with varying compositions: (a) 2/1:2:95 (mol %); (b) 4/2:2:92 (mol %); (c) 6/3:2:89 (mol %); (d) 8/4:2:86 (mol %), and (e) 10/5:2:83 (mol %).

NOVA-1000 nitrogen gas sorption analyzer at the temperature of liquid nitrogen. Glass samples of approximately 0.1 g were degassed at 250 °C for a minimum of 5 h under vacuum. A five point Brunauer-Emmett-Teller (BET) analysis was used to determine the surface area. Data from thermogravimetric analysis (TGA) and differential thermal analysis (DTA) were obtained with a Thermoplus-2 (TG-8120, RIGAKU) analyzer under a nitrogen flow of 5 mL/min. Glass samples of approximately 10 mg were heated from 30 to 800 °C at a rate of 10 °C/min. Fourier transform infrared (FTIR) spectra were recorded (spectral range 600–4000  $cm^{-1}$ , 50 scans, and a resolution of 2  $cm^{-1}$ ) with a JASCO FTIR-460 spectrometer on crushed powders of the glass. The hydrogen permeability of the glass composite membrane (0.52 mm thick) was examined in the range 30–110 °C using a forced convection drying oven (DO-600FA). The proton conductivities of the glass materials were measured on glass pieces with thicknesses of 0.3–1.1 mm, and the two sides these pieces were sputtered with a conducting silver paste to ensure a proper electrical contact.

Polarization measurements were carried out on the MEAs with a Solartron SI 1287 electrochemical interface and a Solartron SI 1260, impedance/gain-phase analyzer. The fuel cell employed for the experiments was a single cell, and the tests were performed with a cell temperature of 28 °C and a RH of 30% at 1 atm of pressure and flow rates of hydrogen and oxygen of 30–50 mL/min into the anode and cathode sides, respectively.

## Results and Discussion

**Pore Study.** Specific surface areas and pore-size distributions were determined from  $N_2$  adsorption/desorption isotherms as shown in Figure 1. The isotherms were of type IV and were characteristic of mesoporous materials. High pore volumes and large pore sizes have been achieved at the calcination temperature of 600 °C. All isotherms displayed a reversible part at low pressure and a hysteresis loop at higher pressures. The shapes of the reversible parts as well as those of the hysteresis loops were very similar for all samples.

Table 1 presents the pore sizes and surface area properties of the mixed HPAs (PWA/PMA) incorporated into the  $P_2O_5$ - $SiO_2$  gel matrix. The BET<sup>27</sup> surface areas of the glass membranes along with their average pore diameters calcu-

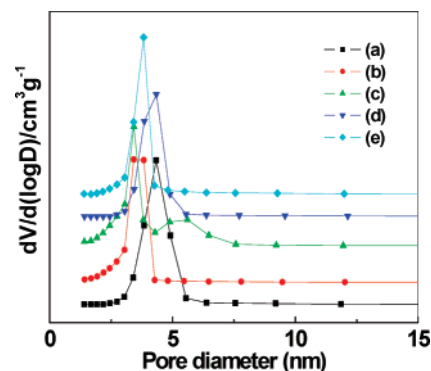


**Figure 2.** Textural properties of PWA/PMA- $P_2O_5$ - $SiO_2$  glass samples (heat treated at 600 °C) with varying compositions: (a) 2/1:2:95 (mol %); (b) 4/2:2:92 (mol %); (c) 6/3:2:89 (mol %); (d) 8/4:2:86 (mol %), and (e) 10/5:2:83 (mol %).

**Table 1.** Textural Characteristics of the PWA/PMA- $P_2O_5$ - $SiO_2$  Glass Composite Membranes

sample no.	compositions (mol %)	average pore size (nm)	average pore volume ( $cm^3/g$ )	specific surface area ( $m^2/g$ )
1	2/1:2:95	5.333	0.238	$178 \pm 2$
2	4/2:2:92	3.768	0.228	$242 \pm 2$
3	6/3:2:89	3.829	0.237	$247 \pm 2$
4	8/4:2:86	5.421	0.188	$139 \pm 2$
5	10/5:2:83	4.532	0.189	$168 \pm 2$

lated according to the Barret-Joyner-Halenda (BJH) method<sup>28</sup> are reported in the table. The pores size distribution was calculated as a function of volume or specific surface area of the pores and presented similar curves for all samples as shown in Figure 2. The pore diameter varied between 3.7 and 5.4 nm for all glass composite membranes for different surface coverages (139–247  $m^2/g$ ), as results from the pore size distribution curves. The average pore size was 4.6 nm. Because the surface area of the glass composite membrane significantly affected the rate of the chemical reaction, its measurement was critical. While the pore volume and the surface area both decreased continuously with increasing concentration of PWA/PMA in the phosphosilicate gels, the shape of the pore size distribution remained basically the same.

**Thermal Study.** The thermal stability was measured mainly by TGA and DTA. Figure 3 shows the TGA and DTA curves for pure PWA and PMA. For pure PWA (Figure 3a), endothermic peaks were observed at 77, 123, 418, 538, and 783 °C, and exothermic peaks were observed at 435, 492, and 637 °C on the DTA curve. For pure PMA (Figure 3b), endothermic peaks could be seen at 52 and 215 °C, and the exothermic peaks could be seen at 282, 559, and 598 °C. From the TGA curve, three weight loss regions could be observed at 134, 390, and 428 °C for pure PWA. Similarly, for pure PMA, a small weight loss region was found at 56 °C, and larger ones were found from 137 to 286 °C, at 430 and at 567 °C.

The acid forms of HPAs are usually obtained with large amounts of water of crystallization, and most of these water molecules are released below 100 °C. Decomposition, which takes place at 350–600 °C, is believed to occur according

(27) Brunauer, S.; Emmett, P. H.; Teller, E. *J. Am. Chem. Soc.* **1937**, *59*, 1553.

(28) Barrett, E. P.; Joyner, L. G.; Halenda, P. P. *J. Am. Chem. Soc.* **1951**, *73*, 373.



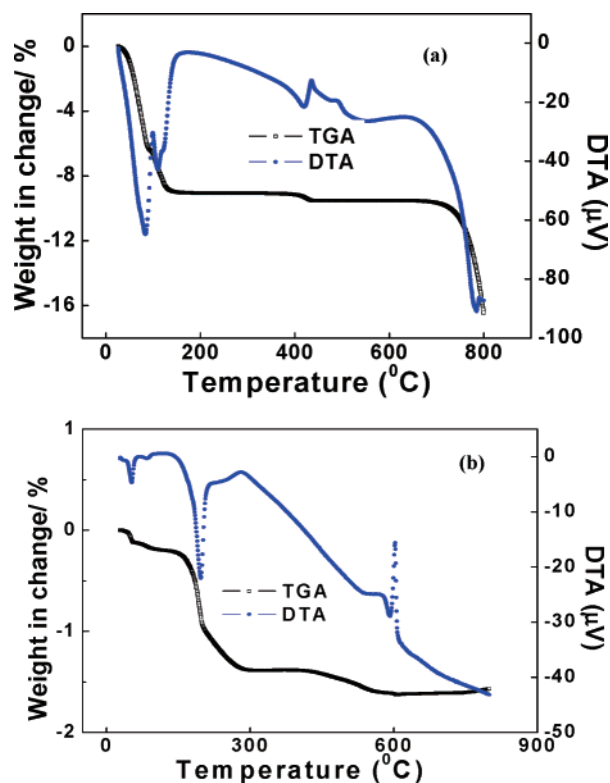
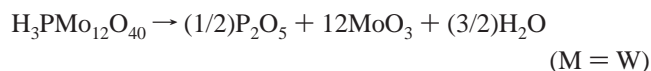


Figure 3. TGA/DTA curves for (a) pure PWA and (b) pure PMA.

to



Hodnett and Moffat assumed that this decomposition proceeded via  $\text{PW}_{12}\text{O}_{38}$  in the case of  $\text{H}_3\text{PW}_{12}\text{O}_{40}$ .<sup>29</sup> The thermal stability also depends on the environment; in a reducing atmosphere heteropoly compounds decompose more rapidly. The coexistence of oxygen and water vapor enhances the stability at high temperatures and sometimes causes the reformation of the heteropoly structure from a decomposed mixture.<sup>30</sup> The FTIR band corresponding to  $\text{Mo(W)}=\text{O}_t$  shifts to a higher wave number, probably due to a loss of hydrogen bonding between  $\text{O}_t$  and water.<sup>31</sup> The peak intensity and bandwidth of P—O and  $\text{Mo(W)}=\text{O}$  change, also probably due to a loss of hydrogen bonding.

Figure 4 displays TGA plots of PWA/PMA— $\text{P}_2\text{O}_5$ — $\text{SiO}_2$  materials with varying compositions. The glass composite membranes exhibited two hydrate loss steps at temperatures of  $\sim 60$  °C and  $\sim 350$  °C as shown in the figure, and these were the two main weight-loss steps in the TGA curve. There was a small weight loss from room temperature to 60 °C, but the quick weight loss started near 100 °C and was attributed to the condensation of phosphoric acid doped in the membranes. The sol–gel mixture was able to stabilize the crystalline water (from 100 to 300 °C). The 350 °C water loss was probably due to dehydration from  $\text{Si}(\text{OH})_4$  to  $\text{SiO}_2$ . It was found that the mixed HPA glass composite membranes

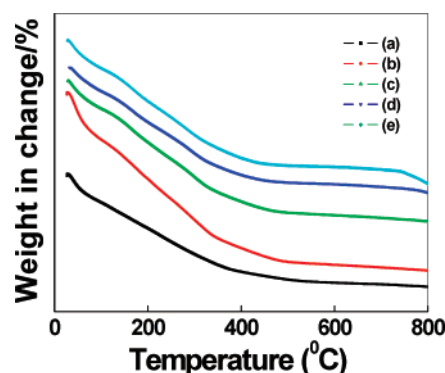


Figure 4. TGA plots of PWA/PMA— $\text{P}_2\text{O}_5$ — $\text{SiO}_2$  glass sample with varying compositions: (a) 2/1:2:95 (mol %); (b) 4/2:2:92 (mol %); (c) 6/3:2:89 (mol %); (d) 8/4:2:86 (mol %), and (e) 10/5:2:83 (mol %).

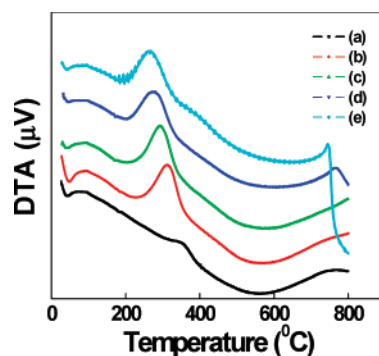


Figure 5. DTA curves for PWA/PMA— $\text{P}_2\text{O}_5$ — $\text{SiO}_2$  glass sample with varying compositions: (a) 2/1:2:95 (mol %); (b) 4/2:2:92 (mol %); (c) 6/3:2:89 (mol %); (d) 8/4:2:86 (mol %), and (e) 10/5:2:83 (mol %).

were stable up to 400 °C. The stability was maintained along a ramp up to 800 °C, except for part of the crystalline water being lost.

In the DTA curves of the same samples (Figure 5), a small endothermic peak was observed at around 50 °C as well as an exothermic peak at 266 °C for the PWA/PMA— $\text{P}_2\text{O}_5$ — $\text{SiO}_2$  glass composite with the composition 2/1:2:95 (mol %; Figure 5a). The latter peak was shifted to higher temperature, that is, from 266 to 346 °C, for increasing PWA/PMA concentrations in the composites (Figure 5b–e). The endothermic peak located around or just below 100 °C was due to the loss of physisorbed  $\text{H}_2\text{O}$  molecules from the surface of the pores in the glass gels. Furthermore, new exothermic peaks at 749 and 766 °C were observed in the DTA curves (Figure 5a,b), and these peak were ascribed to the removal of constitutional water. The results from TGA and DTA demonstrated the presence of two types of water in the heteropoly compounds, that is, crystallization water and “constitutional” water molecules.<sup>32</sup> Loss of the former usually occurs at temperatures below 200 °C. For  $\text{H}_3\text{PMo}_{12}\text{O}_{40}$  and  $\text{H}_3\text{PW}_{12}\text{O}_{40}$ , the constitutional water molecules (acidic protons bound to the oxygen of the polyanion) were lost at temperatures exceeding 270 and 350 °C, respectively. The thermal stability of the HPAs depends strongly on the water evaluation, and numerous studies have reported on certain new supports increasing the HPA stability. Because it seems that the interaction between the Keggin anion and

(29) Uda, T.; Haile, S. M. *Electrochem. Solid State Lett.* **2005**, *8*, A245.

(30) Hodnett, B. K.; Moffat, J. B. *J. Catal.* **1984**, *88*, 253.

(31) Konishi, Y.; Sakata, K.; Misono, M.; Yoneda, Y. *J. Catal.* **1982**, *77*, 169.

(32) Eguchi, K.; Yamazoe, N.; Seiyama, T. *Nippon Kagaku Kaishi* **1981**, *42*, 336.

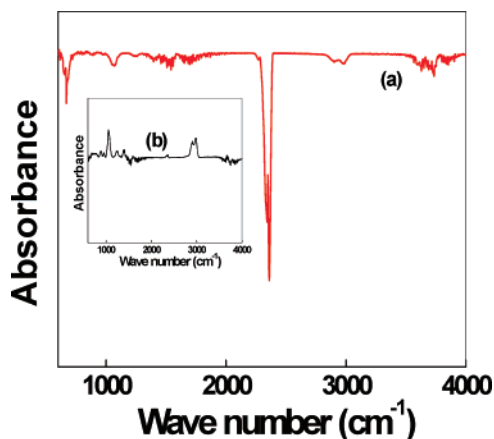


Figure 6. FTIR spectra for (a) pure PWA and (b) pure PMA.

the support occurs through shared protons, it was of the utmost important to determine the HPA protonation sites.

**FTIR Study.** FTIR spectroscopy, as a means of providing the structure of the HPAs, is one of the most important tools in deciding which HPAs will give the best results when used as an electrolyte in fuel cell tests. The method is convenient and widely used for the characterization of heteropolyanions. Additional information about the thermal stability as well as about the structure of the supported HPAs was obtained by FTIR spectroscopy. IR spectra of pure HPAs display specific absorption bands corresponding to the Keggin structure at 1064, 965, 864, and 805  $\text{cm}^{-1}$ , and these are assigned to the stretching vibrations  $\nu_{\text{as}}(\text{P}-\text{O})$ ,  $\nu_{\text{as}}(\text{Mo}=\text{O})$ ,  $\nu_{\text{as}}(\text{Mo}-\text{O}-\text{Mo})$ , and  $\nu_{\text{as}}(\text{Mo}-\text{O}-\text{O}-\text{Mo})$ , respectively.<sup>33,34</sup> The P-O stretching band for  $\text{PW}_{11}\text{O}_{39}^{7-}$  is split into 1085 and 1040  $\text{cm}^{-1}$ .<sup>33</sup> IR spectra of hydrated  $\text{H}_3\text{PW}_{12}\text{O}_{40}$  include a broad OH stretching band and two OH bending bands, at 1610 and 1720  $\text{cm}^{-1}$ . The latter two correspond to water and protonated water, respectively.<sup>35</sup> IR studies to date<sup>36-43</sup> have mostly concerned Keggin acids and their salts, and infrared measurements have mostly been used for elucidating structural relationships between heteropolyanions.

The main IR bands for pure PWA and PMA can be seen in Figure 6a,b, respectively. Peaks at the wave numbers 727, 879, 942, 1056, 1259, 1399, 1615, 2896, 2972, 3669, and 3758  $\text{cm}^{-1}$  indicate the existence of PMA (Figure 6a), and peaks at 625, 753, 971, 1077, 1312, 1531, 1699, 2337, 2895, 3483, 3669, and 3928  $\text{cm}^{-1}$  indicate that of PWA (Figure 6b). Figure 7 portrays the IR spectra for the composite membranes with varying composition, and the

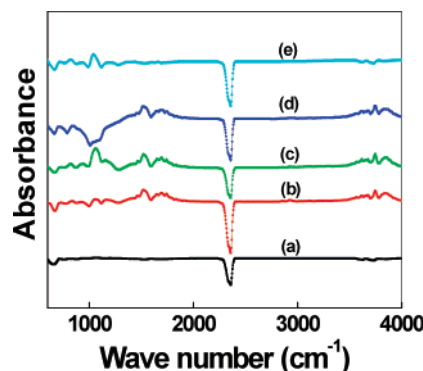


Figure 7. FTIR spectra of PWA/PMA- $\text{P}_2\text{O}_5$ - $\text{SiO}_2$  glass sample with varying compositions: (a) 2/1:2:95 (mol %); (b) 4/2:2:92 (mol %); (c) 6/3:2:89 (mol %); (d) 8/4:2:86 (mol %), and (e) 10/5:2:83 (mol %).

peaks at 667, 790, 983, 1130, 1594, 1724, 2352, 2935, 3652, and 3779  $\text{cm}^{-1}$  indicate the incorporation of HPAs in the phosphosilicate glass. In addition, there were several very strong bands below 1122  $\text{cm}^{-1}$  due to the presence of PWA. It was found that the wave numbers of PWA in the glass membranes were shifted away from those of pure PWA by a few inverse centimeters, indicating that the Keggin geometry of PWA was preserved inside the membranes. The bands of  $\text{W}-\text{O}_b-\text{W}$  and  $\text{W}-\text{O}_c-\text{W}$  both display blue shifts. Rocchiccioli-Deltcheff et al.<sup>33</sup> correlated the wave number shifts of the  $[\text{W}-\text{O}_d-\text{W}]$ ,  $[\text{W}-\text{O}_c-\text{W}]$ , and  $[\text{W}-\text{O}_b-\text{W}]$  bands with the strength of anion-anion interactions, which take place as a result of the electrostatic repulsion between the PW anions in the crystalline compounds. They proposed that, with increasing anion-anion interactions as a result of the increasing distance between the oxygens of the neighboring PW anion, the pure stretching  $[\text{W}-\text{O}_d]$  band would exhibit a decrease in its wave number. The opposite shifts were proposed for the other two vibrations because of their mixed bend stretching character.

The shifts of the PWA/PMA- $\text{P}_2\text{O}_5$ - $\text{SiO}_2$  glass membrane were larger than that of pure PMA or pure PWA: the reason probably being that the electrostatic repulsion between the Keggin ions in PWA and PMA were likely to be smaller than that in the glass composite membrane. The absorption band at 813  $\text{cm}^{-1}$  was assigned to the bending mode of the silanol groups,<sup>34</sup> and the peaks at 879, 836, 875, and 848  $\text{cm}^{-1}$  (Figure 7a-e) were assigned to the stretching mode of the  $\text{W}-\text{O}-\text{W}$  ( $\text{W} = \text{M}$ ) bonds;<sup>35</sup> however, the peaks at 960, 983, and 987  $\text{cm}^{-1}$  were due to the stretching vibrations of  $\text{W} = \text{O}$  in the Keggin structure (Figure 7a-e).<sup>35</sup> Further peaks typical of the Keggin structure (i.e., the asymmetric stretching vibration of the central  $\text{PO}_4$  tetrahedron) at 1064 and 1099  $\text{cm}^{-1}$  were partially overlaid by the Si-O frame vibrations.<sup>35</sup> It appears that the molecular structure of PWA was retained after adsorption on the silica surface. The most important features for the filler applications in the glass composite membranes were related to the adsorption properties of water on the surface.

**Permeability Study.** Figure 8 shows the hydrogen permeability of the PWA/PMA- $\text{P}_2\text{O}_5$ - $\text{SiO}_2$  (2/1:2:95 mol %) glass composite membrane. The permeation tests were carried out in the temperatures range of 30–110  $^{\circ}\text{C}$ . The glass membrane displayed an activated transport of all gases which

- (33) Rocchiccioli-Deltcheff, C.; Fournier, M.; Franck, R.; Thouvenot, R. *Inorg. Chem.* **1983**, 22, 207.
- (34) Bridgeman, A. J. *Chem. Phys.* **2003**, 287, 55.
- (35) (a) Chen, N.; Yang, R. T. *J. Catal.* **1995**, 76, 157. (b) Sundholm, F. *Proceedings of the 9th International Conferences on Solid state Protonic conductors SSPC'98, Extended Abstracts*, Bled, Slovenia, Aug 17–21, 1998; Kluwer Academic Publisher: Norwell, MA, 1998; p 155.
- (36) Tsigdinos, G. A.; Hallada, C. J. *Inorg. Chem.* **1968**, 7, 437.
- (37) Flynn, C. M.; Pope, M. T. *Inorg. Chem.* **1971**, 10, 2745.
- (38) Flynn, C. M.; Pope, M. T. *Inorg. Chem.* **1972**, 11, 1950.
- (39) Flynn, C. M.; Pope, M. T. *Inorg. Chem.* **1971**, 10, 2524.
- (40) Sharpless, N. E.; Munday, J. S. *Anal. Chem.* **1957**, 29, 1619.
- (41) Brown, D. H. *Spectrochim. Acta* **1963**, 19, 585.
- (42) Bakhchisaraitseva, S. A.; Kabanov, V. Y.; Spitsyn, V. I. *Dokl. Akad. Nauk SSSR* **1967**, 174, 614.
- (43) Rabette, P.; Olivier, D. *Rev. Chim. Miner.* **1970**, 7, 181.

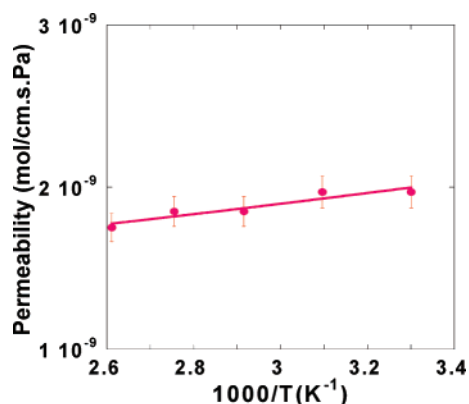


**Figure 8.** Permeability rate as a function of the inverse temperature under a hydrogen feed for the PWA/PMA–P<sub>2</sub>O<sub>5</sub>–SiO<sub>2</sub> (2/1:2:95 mol %) glass membrane.

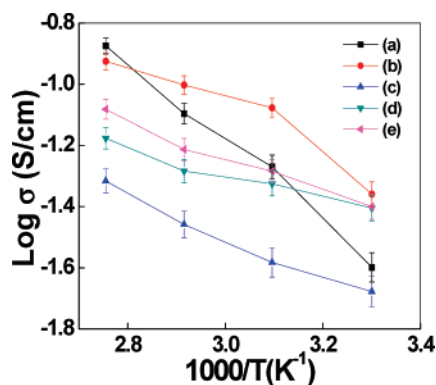


**Figure 9.** Arrhenius plot displaying the logarithm conductivity against the inverse temperature for PWA/PMA–P<sub>2</sub>O<sub>5</sub>–SiO<sub>2</sub> glass composite membranes with varying compositions: (a) 2/1:2:95 (mol %); (b) 4/2:2:92 (mol %); (c) 6/3:2:89 (mol %); (d) 8/4:2:86 (mol %), and (e) 10/5:2:83 (mol %).

decreased with temperature as the permeation increased as a function of temperature. These results strongly indicate that the membranes were of a high quality without pin holes or microcracks. Otherwise, Pouisselle or Knudsen diffusion would dominate the molecular transport resulting in the gas permeation decreasing with temperature. The translational diffusion of the gas better explains the transport *minima or maxima* observed at lower and higher temperatures.<sup>44</sup> Transport of molecules through the glass pores occurs by transfer from the gas phase within large pores or surface adsorbed sites. However, surface diffusion plays only a minor role (<2%) on the total transport mechanism in silica materials.<sup>45</sup> The hydrogen permeability of the glass composite membrane at 30 °C was measured to  $1.97 \times 10^{-9}$  cm<sup>2</sup>/s, and the permeability value of  $1.75 \times 10^{-9}$  cm<sup>2</sup>/s was decreased with increasing temperature up to 110 °C. This value was higher than that of a Nafion membrane, which showed a hydrogen permeability of  $3.01 \times 10^{-13}$  cm<sup>2</sup>/s at 30 °C when measured in our laboratory.

**Proton Conductivity.** HPAs exist in a series of hydrated phases, of which the stable forms depend strongly on temperature and RH. Figure 9 portrays the temperature dependence of the conductivity, in an Arrhenius plot of the logarithm of the conductivity against the inverse temperature.

The conductivity was measured in the temperature range from 30 to 90 °C at 70% RH. The maximum high proton conductivity was found to be 0.13 S cm<sup>-1</sup> at 90 °C for the PWA/PMA–P<sub>2</sub>O<sub>5</sub>–SiO<sub>2</sub> (2/1:2:95 mol %) composite. This result was comparable with previous research based on these two clusters, which yielded an excellent proton conductivity of 0.17 S cm<sup>-1</sup> at room temperature.<sup>46</sup> Concerning the glass composite membranes, the conductivity increased with increasing amounts of PWA and PMA, suggesting that the hydrolysis and polymerization proceeded slowly under the experimental conditions. However, the conductivity increase was not significant with respect to the PWA and PMA concentration as can be seen in Figure 9b,c. The conductivity was approximately  $4.8 \times 10^{-2}$  S cm<sup>-1</sup> at 90 °C for a PWA/PMA content of 6/3 mol %, which was lower than the corresponding value for the 4/2 mol % sample. Increasing the PWA/PMA content further rendered systematic increases in conductivity, however, never reaching the values of the 4/2 mol % sample. This can be explained by the simplest model of glass structure, Zachariasen's continuous random network model that represents glasses as being formed by a random orientational disorder of bond angles. Correspondingly, the simple Rasch–Henderson equation,  $\log \sigma = A - B/T$ , has been used to describe conductivity.<sup>47</sup> There are, however, a series of reports indicating that glasses and glass electrolytes in particular are inhomogeneous on a 1–10 nm scale. The nature of the conduction mechanism can vary from hopping in a disordered random network potential<sup>48–50</sup> to a percolation pathway involving higher mobilities in a particular region of an inhomogeneous glass, with slower motions in the intervening structure.<sup>51</sup>

Although the conductivity difference among the composites was not large, it was evident that the addition of a mixture of PWA and PMA was an effective means of increasing the conductivity. The high conductivity values were expected as a result of the high proton loading levels. It is also known that these clusters could be functionalized much more easily than the PWAs or the PMA.

**H<sub>2</sub>/O<sub>2</sub> Fuel Cell Test.** Polarization curves are obtained during the testing of an electrolyte, and a typical polarization curve can be seen in Figure 10. This figure presents the current versus voltage, for a gradual voltage decrease. The voltage drop is the straight forward resistance to the flow of electrons through the material of the electrodes and the various interconnections, as well as the resistance to the flow of ions through the electrolyte. The polarization data were obtained after 10 h of cell operation at a temperature of 28 °C and a hydrogen and oxygen gas pressure of 1 atm. It can be observed that a current density of 137 mA/cm<sup>2</sup> was obtained at a cell voltage of 0.5 V. The power density was

(44) Gilron, J.; Soffer, A. *J. Membr. Sci.* **2002**, 209, 339.

(45) De Lange, R. S. A.; Keizer, K.; Burggraaf, A. J. *J. Membr. Sci.* **1995**, 104, 81.

(46) Nakamura, O.; Kodama, T.; Ogino, I.; Miyake, Y. *Chem. Lett.* **1979**, 1, 17.

(47) Ravaine, D.; Souquet, J. L. In *Solid Electrolytes*; Hagenmuller, P., Van Gool, W., Eds.; Academic Press: New York, 1978; Chapter 17 Mat. Sci. Ser.

(48) Pechenik, A.; Susman, S.; Whitmore, D. H.; Ratner, M. A. *Solid State Ionics* **1986**, 18/19, 403.

(49) Ratner, M. A.; Schriver, D. F. *Chem. Rev.* **1988**, 88, 109.

(50) Ratner, M. A.; Nitzan, A. *Solid State Ionics* **1988**, 28–30, 3.

(51) Malugani, J. P.; Tachez, M.; Mercier, R.; Dianoux, A. J.; Chieux, P. *Solid State Ionics* **1987**, 23, 189.

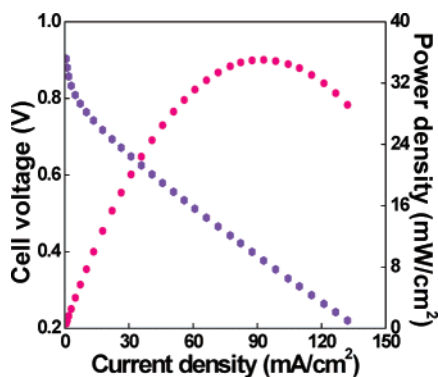


**Figure 10.** Polarization curve displaying the current density and power density for the PWA/PMA- $\text{P}_2\text{O}_5$ - $\text{SiO}_2$  (2/1:2:95 mol %) glass membrane at room temperature.

$\sim 35 \text{ mW/cm}^2$  at  $93 \text{ mA/cm}^2$  for the PWA/PMA- $\text{P}_2\text{O}_5$ - $\text{SiO}_2$  (2/1:2:95 mol %) glass composite membrane and the  $0.1 \text{ mg/cm}^2$  Pt/C electrode. The measured internal resistance of the fuel cell before the polarization test was  $3.5 \Omega \text{ cm}^2$ . The high conductivity value of the electrolyte and the relatively thin matrix could justify the improvement in results as compared to those obtained by Nakamura et al. on solid electrolytes utilized in fuel cells.<sup>52,53</sup>

After the fuel cell test, a color change from white to blue on the electrolyte surface surrounding the electrode area could be observed. A feature of heteropoly blue formation is the rapid and reversible reduction process.<sup>54</sup> Polyanions that form heteropoly blues have polargrams with several reversible diffusion-controlled waves. It therefore follows that reduction must be accompanied by only minor structural changes. This can be achieved if the  $\text{MO}_6$  octahedra of which the polyanion is constructed each have one terminal oxygen atom, because an electron added to M enters an orbital that

is predominantly nonbonding, with minimal subsequent bond length alteration. This electrochemical reduction of the tungsten-containing polyanion would render it suitable for use in displays or as inorganic resists.<sup>55</sup>

## Conclusion

New, highly proton conductive glass composite membranes consisting of phosphosilicate gels doped with a mixture of PWA and PMA HPAs and to be utilized for  $\text{H}_2/\text{O}_2$  fuel cells were fabricated by a sol-gel method. To enhance the proton conductivity ( $\sigma$ ) of these glass membranes,  $0.134 \text{ S cm}^{-1}$  was obtained for  $90^\circ\text{C}$  and 70% RH and  $1.014 \text{ S cm}^{-1}$  was obtained for  $85^\circ\text{C}$  and 85% RH. The porous glasses (with average pore sizes below 6 nm) were thermally stable up to  $200^\circ\text{C}$ . New proton conducting membranes were prepared utilizing several of the most thermally stable glass systems such as the PWA and PMA. The hydrogen permeability was found to decrease in the temperature range 30 to  $110^\circ\text{C}$ , going from  $1.97 \times 10^{-9}$  to  $1.75 \times 10^{-9} \text{ cm}^2/\text{s}$ . A maximum output value of  $35 \text{ mW/cm}^2$  and a current density of  $137 \text{ mA/cm}^2$  were obtained at  $28^\circ\text{C}$  when using this novel glass composite membrane in fuel cell tests. A maximum performance was achieved for the PWA/PMA: $\text{P}_2\text{O}_5$ : $\text{SiO}_2$  glass composite membrane with a composition of 2/1:2:95 mol % and a Pt/C loaded of  $0.1 \text{ mg/cm}^2$  on the electrodes. Although the present investigation has revealed high proton conductivities of the glass composite membranes at the low temperatures, it is necessary to suppress the reduction of the PWA/PMA component in the glass composite during fuel cell operation.

**Acknowledgment.** The authors wish to thank the Japan Society for the Promotion of Science (JSPS) fellowship program for the financial support for this research.

CM070567F

- (52) Nakamura, O. *Prog. Batteries Sol. Cells* **1982**, 4, 230.  
 (53) Nakamura, O.; Ogino, I.; Kodama, T. In *Hydrogen Energy Progress: Proceeding of the 3rd World Hydrogen Energy Conferences*, Tokyo, Japan, June 23–26, 1980; p 119.  
 (54) Giordano, N.; Staiti, P.; Arico, A. S.; Passalacqua, E.; Abate, L.; Hocevar, S. *Electrochim. Acta* **1997**, 42, 1645.

- (55) Tatsumisago, M.; Minami, T. *J. Am. Ceram. Soc.* **1989**, 72, 484.